

Measurement of the $1s2p\ ^3P_0 - ^3P_1$ Fine Structure Interval in Helium-Like Magnesium

E.G. Myers¹ and M.R. Tarbutt²

¹ Department of Physics, Florida State University, Tallahassee,
Florida 32306-4350, USA

² Clarendon Laboratory, University of Oxford, Oxford OX1 3PU, UK

Abstract. Using Doppler-tuned fast-beam laser spectroscopy the $1s2p\ ^3P_0 - ^3P_1$ fine structure interval in $^{24}\text{Mg}^{10+}$ has been measured to be $833.133(15)\text{ cm}^{-1}$. The calibration procedure used the intercombination $1s2s\ ^1S_0 - 1s2p\ ^3P_1$ transition in $^{14}\text{N}^{5+}$. The result tests quantum-electrodynamic and relativistic corrections to high precision calculations, which will be used to obtain a new value for the fine structure constant from the fine structure of helium.

1 Introduction

Precision spectroscopy of two-electron atoms tests fundamental relativistic and quantum-electrodynamic atomic theory. Additional current interest in helium-like $1s2p\ ^3P$ fine structure stems from the possibility of obtaining the fine structure constant, α , from comparison of theory [1,2,3] and experiment [4,5,6,7,8,9] for the fine structure of helium. Measurements in moderate Z ions, though less precise than those in helium, can be more sensitive to higher-order relativistic and QED corrections. Measurements have been carried out using laser techniques in Li^+ , see *e.g.* ref. [10], Be^{2+} [11], B^{3+} [12], N^{5+} [13,14], and F^{7+} [15,16]. For higher Z , fine structure intervals have been obtained from VUV emission spectroscopy of the $1s2p\ ^3P_J - 1s2s\ ^3S_1$ transitions, but only of the $J = 0 - J = 2$ interval for $Z > 12$, see *e.g.* [17,18]. For $Z = 47$ [19] and 64 [20], $0 - 1$ measurements have been obtained indirectly from the hyperfine-quenched lifetime of the 2^3P_0 state. Here we report the extension of laser techniques to the direct measurement of the $1s2p\ ^3P_0 - ^3P_1$ fine structure transition at $Z = 12$ [21]. The precision obtained, better than 20 ppm, provides an exacting test of higher-order relativistic and QED corrections.

2 Method

The relevant energy levels of Mg^{10+} are shown in fig. 1. The experimental arrangement, see fig. 2, was similar to that described in refs. [14,15]. A nominally 50.3 MeV beam of $^{24}\text{Mg}^{6+}$, $v/c \simeq 0.067$, was obtained from the Florida State University tandem electrostatic accelerator and momentum analyzed in a 90° bending magnet. The analyzed beam, current 5-10 particle-nA, was focused to a diameter of approx. 1.25 mm and passed through a 4 or 10 $\mu\text{g cm}^{-2}$ carbon foil in

the interaction chamber, for further stripping and excitation. After the foil, the Mg^{10+} charge-state was magnetically deflected 4.1° , bringing it co-linear with the laser beam. In the ion-laser beam overlap region, 17 cm down-beam of the foil, 1.3 keV X-rays were detected using a proportional counter, operated with pure methane at 500 mbar pressure and fitted with a $1\text{ }\mu\text{m}$ thick polypropylene window. The X-ray count rate in the proportional counter was 30 kHz/particle-nA for the $4\text{ }\mu\text{g cm}^{-2}$ foil, and 50 kHz/particle-nA for the $10\text{ }\mu\text{g cm}^{-2}$ foil.

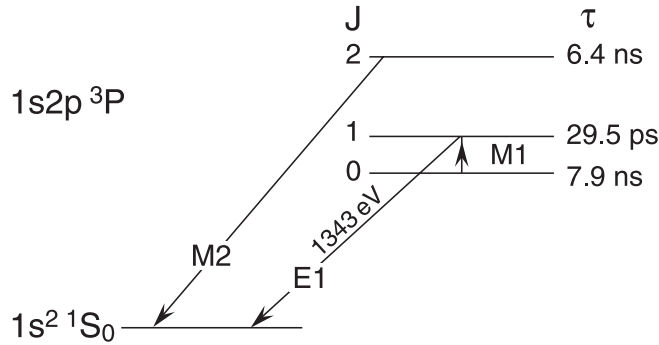


Fig. 1. Energy levels of Mg^{10+} relevant to the experiment

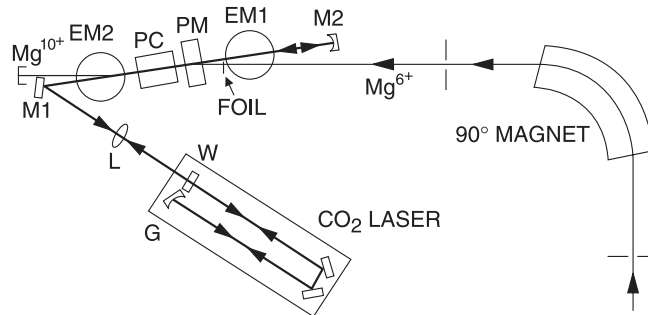


Fig. 2. Schematic of the experimental arrangement. G is a diffraction grating, W a window, L a lens, $M1$ and $M2$ are mirrors, PC is a proportional counter, PM is a permanent magnet, and $EM1$ and $EM2$ are electromagnets

Details of the continuous wave, axial flow, line tunable, extended cavity CO_2 laser system, and of our alignment procedure, are given in ref. [14]. To access a wavelength near $12.0\text{ }\mu\text{m}$ required operating the laser on the P-branch of the $01^{11} - [11^{10}, 03^{10}]_f$ hot-band of $^{12}\text{C}^{16}\text{O}_2$ [22], and using the laser beam co-propagating with the ion beam. The P-40 line at 890.9408 cm^{-1} was used for most of the data taking. Switching the laser discharge at 500 Hz with a 50%

duty cycle we obtained intracavity powers of 350 W, with a spot-size diameter at the interaction region matched to the ion beam. At the peak of the Mg^{10+} resonance the laser induced X-ray signal was 3×10^{-3} of the X-ray background.

3 Allowance for Doppler Shift

The fine structure interval ΔE_{01} is obtained from the laser wavenumber and the ion beam velocity using the relativistic Doppler formula. To calibrate the 90° analysing magnet we tuned a $^{14}\text{N}^{3+}$ beam from the tandem accelerator, through the 90° magnet, and through the same foil in the interaction chamber, and induced the $\text{N}^{5+} 1s2s\ ^1\text{S}_0 - 1s2p\ ^3\text{P}_{1,F=2}$ intercombination transition with the CO_2 laser. Detection was via the 426 eV X-ray decay of the $^3\text{P}_1$ level to the ground state, using the same proportional detector, but operated at 300 mbar for increased gain. The wavenumber of this intercombination transition has been measured to be $986.0062(7)\text{ cm}^{-1}$ [14], and hence the velocity of the N^{5+} beam at the center of the resonance is well determined. With the normal band P-34 CO_2 line at 931.0014 cm^{-1} [23], this resonance occurs at a beam energy near 21.5 MeV. At this energy the $^{14}\text{N}^{3+,5+}$ beams have similar magnetic rigidities to the 50.3 MeV $^{24}\text{Mg}^{6+,10+}$ beams, respectively. Hence they are transmitted through the 90° analysing magnet at similar B-fields, and take similar paths through the fixed magnetic field in the interaction chamber.

It is convenient to work in terms of the quantity $p = \beta\gamma$, where $\beta = v/c$, and $\gamma = (1 - \beta^2)^{-1/2}$. In our situation, by relating the rigidities of the two beams transmitted through the analysing magnet, the $\beta\gamma$'s of the two resonances are related by,

$$p(\text{Mg}^{10+}) = 2 \frac{M_N}{M_{\text{Mg}}} p(\text{N}^{5+}) + 6 \frac{M_H}{M_{\text{Mg}}} \frac{dp(H^+)}{dB} [B(\text{Mg}) - B(\text{N})] \\ + 2 \frac{M_N}{M_{\text{Mg}}} \Delta p(\text{N}) - \Delta p(\text{Mg}) \quad (1)$$

where M_N , M_{Mg} , and M_H are the masses of the $^{14}\text{N}^{3+}$ and $^{24}\text{Mg}^{6+}$ ions, and of the proton; $B(\text{Mg})$ and $B(\text{N})$ are the magnetic fields corresponding to the resonance centroids; $dp(H^+)/dB$ is the differential magnet calibration constant determined from a well known $^{12}\text{C}(p, p')^{12}\text{C}$ nuclear resonance; and $\Delta p(\text{N})$ and $\Delta p(\text{Mg})$ are the losses in $\beta\gamma$ for the two beams due to kinetic energy lost in the foil.

4 Doppler-tuned Resonances

Fig. 3 shows the combined Mg^{10+} data, and N^{5+} resonances obtained with the same $4\text{ }\mu\text{g cm}^{-2}$ foil. The magnesium resonance width is dominated by the natural width due to the 29.5 ps mean lifetime of the $2\ ^3\text{P}_1$ state [24]. A Lorentzian fit gave a FWHM in beam energy of 315(24) keV, consistent with the 326 keV expected from the natural width. The widths of the much narrower nitrogen

resonances are dominated by the distribution of energy loss in the foil. Fits to simple Gaussians of the combined up and down scan resonances gave FWHM's of 20(1) keV before, and 22(1) keV after, the magnesium run.

5 Results

Using centroids obtained from the fits, together with eqn. 1 and the relativistic Doppler formula, our result for the $^{24}\text{Mg}^{10+} \ 3\text{P}_0 - 3\text{P}_1$ fine structure interval is $\Delta E_{01} = 833.133(15) \text{ cm}^{-1}$. The contributions to the final error are shown in table 1. The largest contribution is from the estimate of the difference of the actual, non-equilibrium, energy loss in the thin foil, and the standard, tabulated (thick foil) energy loss data [25].

Table 1. Contributions to the error in the measurement of the $^{24}\text{Mg}^{10+} \ 2^3\text{P}_0 - 2^3\text{P}_1$ fine structure interval. Units are 10^{-3} cm^{-1}

statistical	3
foil thickness	0.9
tabulated stopping power	2.1
non-equilibrium stopping power	12
ion, laser beam overlap	5
angular misalignment, laser divergence	4
average laser frequency	0.1
N^{5+} wavenumber	0.6
trajectory in 90° magnet	3
90° magnet differential calibration	0.3
total	14.5

In table 2 our result is compared with the UV spectroscopic result of Klein *et al.* [26]. Also shown are the theoretical results of Zhang *et al.* [2], Plante *et al.* [27], and Chen *et al.* [28]. The first of these uses perturbation theory, with matrix elements of effective operators derived from the Bethe-Salpeter equation, evaluated with high precision solutions of the non-relativistic Schrödinger equation. This yields a power series in α and $\ln \alpha$. The calculations of Zhang *et al.* include terms up to $O(\alpha^5 \ln \alpha)$ but omit terms of $O(\alpha^5)$ a.u. The calculations of Plante *et al.* use an “all orders” relativistic perturbation theory method, while those of Chen *et al.* use relativistic configuration interaction theory. These both obtain all “structure” terms, up to $(Z\alpha)^4$ a.u., and use explicit QED corrections from Drake [29].

In fig. 4 we plot the differences between the results of precision experiments and theory for the $2^3\text{P}_0 - 2^3\text{P}_1$ and $2^3\text{P}_1 - 2^3\text{P}_2$ intervals of helium-like ions for

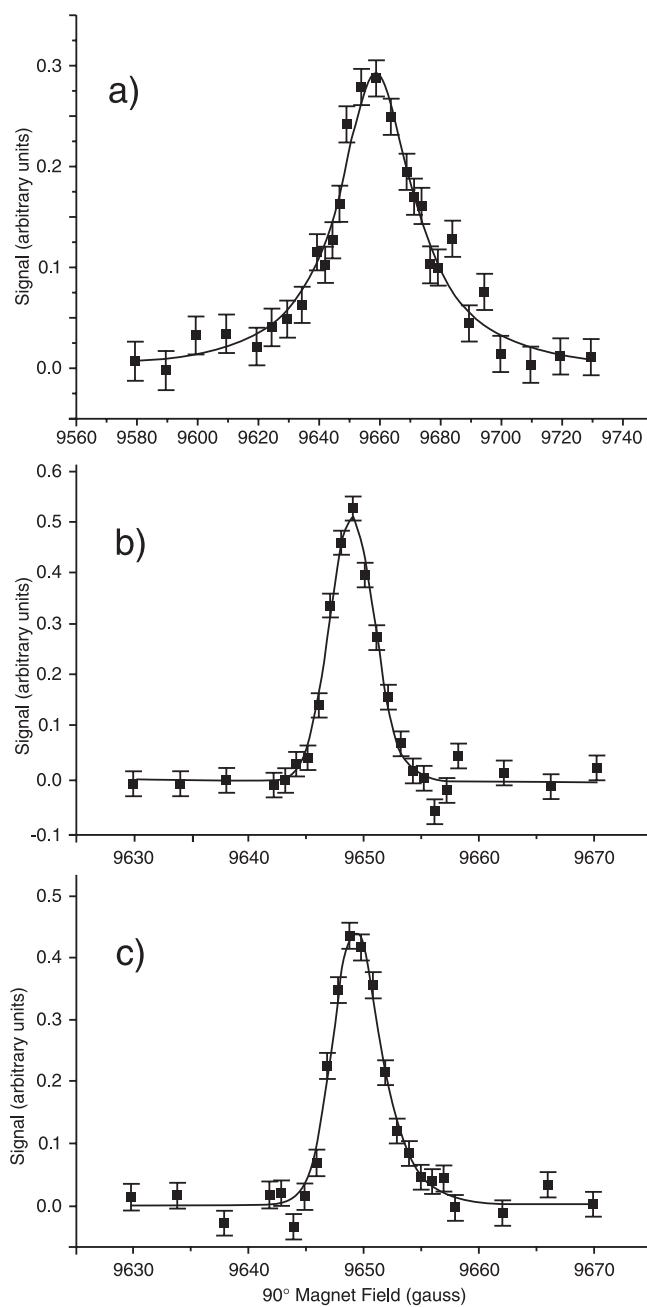


Fig. 3. Doppler tuned resonances of (a) the $^{24}\text{Mg}^{10+} 2\ ^3\text{P}_0 - 2\ ^3\text{P}_1$ fine structure transition, and of the $^{14}\text{N}^{5+} 2\ ^1\text{S}_0 - 2\ ^3\text{P}_{1,F=2}$ intercombination interval, obtained (b) before, and (c) after, the magnesium data. All resonances were obtained with the same $4\ \mu\text{g cm}^{-2}$ carbon foil

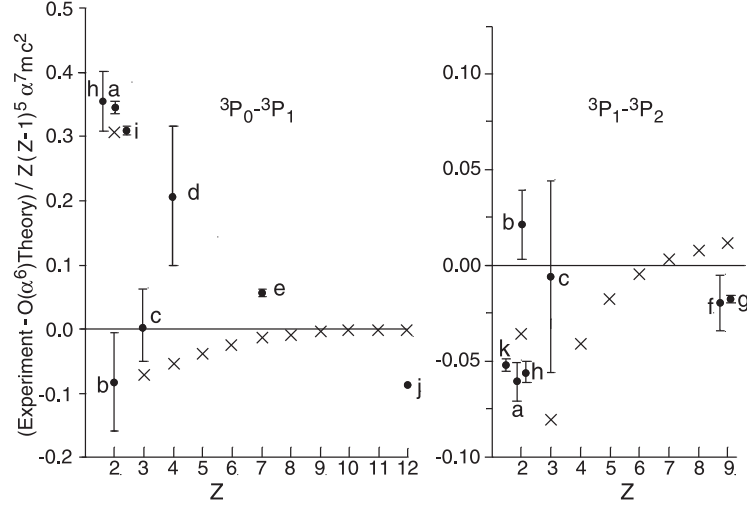


Fig. 4. Results of precision experiments for the $2\ ^3P_0 - 2\ ^3P_1$ and $2\ ^3P_1 - 2\ ^3P_2$ fine structure intervals for $2 \leq Z \leq 12$, compared with the $O(\alpha^6 m_e c^2)$ theory of Yan and Drake [1] (baseline). The $O(\alpha^7 \ln \alpha)$ corrections of Zhang, Yan and Drake [2] are indicated by crosses. The experimental points are as follows: a) Shiner *et al.* [4], b) Lewis *et al.* [30], and Frieze *et al.* [31], c) Riis *et al.* [10], d) Scholl *et al.* [11], e) Thompson *et al.* [14], f) Myers *et al.* [16], g) Myers *et al.* [15], h) Storry *et al.* [5,8], i) Minardi *et al.* [6], j) This work (Myers *et al.* [21]), k) Castilleja *et al.* [9]. On this scale, the error bar for magnesium is contained within the point shown

Table 2. Experimental results for the $^{24}\text{Mg}^{10+}\ 2\ ^3P_0 - 2\ ^3P_1$ fine structure interval compared with recent theory

	$\Delta E_{01}\ (\text{cm}^{-1})$
This experiment	833.133(15)
Previous experiment [26]	832(9)
Zhang, Yan and Drake [2]	832.335
Plante, Johnson, and Sapirstein [27]	833.1
Chen, Cheng, and Johnson [28]	833.3

$Z \leq 12$. For the baseline we take the well established perturbation theory up to $O(\alpha^4)$ [1,3]. The additional terms of $O(\alpha^5 \ln \alpha)$ [2,3] are indicated by crosses. The scaling factor of $Z(Z-1)^5 \alpha^5$ corresponds to the spin-dependent part of the one-electron self-energy for the 2p state [1]. From the figure it can be seen that, while the inclusion of the $O(\alpha^5 \ln \alpha)$ terms greatly improves agreement between theory and recent measurements for helium, it does not do so for higher Z . However, the discrepancies are within the estimated magnitude of the remaining terms of $O(\alpha^5)$ a.u. which are being calculated and checked [32].

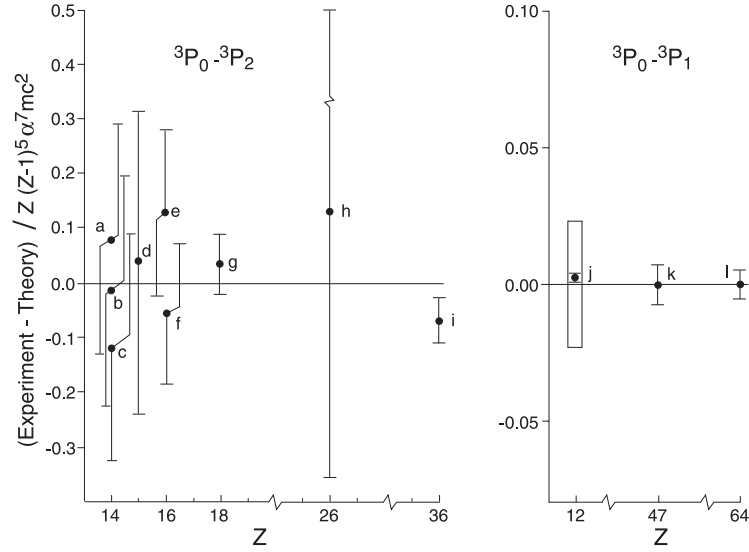


Fig. 5. (a) Results of precise ultra-violet emission spectroscopy for the $2\ {}^3P_0 - 2\ {}^3P_2$ intervals, and (b) present result, and results of hyperfine-quenched lifetime measurements for the $2\ {}^3P_0 - 2\ {}^3P_1$ intervals $Z \geq 12$, compared with the relativistic theory of Plante *et al.* [27] (baseline). Other UV spectroscopic results with significantly larger error bars, when scaled by $Z(Z-1)^5$, e.g. [26], have been omitted for clarity. The experimental points are as follows: a) Howie *et al.* [33], b) Curdt *et al.* [34], c) DeSerio *et al.* [35], d) Howie *et al.* [36], e) Howie *et al.* [17], f) DeSerio *et al.* [35], g) Kukla *et al.* [18], h) Buchet *et al.* [37], i) Martin *et al.* [38], j) This work (Myers *et al.* [21]), k) Birkett *et al.* [19], l) Indelicato *et al.* [20]. The block around point j indicates the theoretical uncertainty corresponding to the number of significant figures given in ref. [27]. Elsewhere the theoretical uncertainty is smaller than the experimental uncertainties

For completeness, in fig. 5 we compare some of the more precise experimental measurements of helium-like $n = 2$ fine structure at higher Z with the “all-orders relativistic perturbation theory” calculations of Plante *et al.* [27]. Fig. 5a

shows the results for $2\ ^3P_2 -\ ^3P_0$ intervals obtained from ultra-violet grating spectroscopy. Fig. 5b shows the results of our laser spectroscopic measurement, and of the two hyperfine-quenched lifetime measurements. As can be seen, all previous experiments, within the experimental error bars, show no significant disagreement with theory. In view of the relatively large numerical rounding error in the theory [27] for $Z = 12$ on the expanded scale in fig. 5b, the excellent agreement with the experimental result is partially coincidental.

6 Acknowledgments

This work was supported by the National Science Foundation (Nuclear Physics), the State of Florida and the NATO CRG program.

References

1. Z.-C. Yan and G.W.F. Drake: Phys. Rev. Lett. **74**, 4791 (1995)
2. T. Zhang, Z.-C. Yan, and G.W.F. Drake: Phys. Rev. Lett., **77**, 1715 (1996)
3. K. Pachucki: J. Phys. B**32**, 137 (1999)
4. D. Shiner, R. Dixon, and P. Zhao: Phys. Rev. Lett. **72**, 1802 (1994); R. Dixon and D. Shiner: Bull. Am. Phys. Soc. **39**, 1059 (1994)
5. C.H. Storry and E.A. Hessels: Phys. Rev. A**58**, R8 (1998)
6. F. Minardi, G. Bianchini, P. Cancio Pastor, G. Giusfredi, F.S. Pavone, and M. Inguscio: Phys. Rev. Lett. **82**, 1112 (1999)
7. C.M. Levy, T.M. Roach and G. Gabrielse: private Communication 1999
8. C.H. Storry, M.C. George, and E.A. Hessels: Phys. Rev. Lett. **84**, 3274 (2000)
9. J. Castilleja, D. Livingston, A. Sanders, and D. Shiner: Phys. Rev. Lett. **84**, 4321 (2000)
10. E. Riis, A.G. Sinclair, O. Poulsen, G.W.F. Drake, W.R.C. Rowley, and A.P. Levick: Phys. Rev. A **49**, 207 (1994)
11. T.J. Scholl, R. Cameron, S.D. Rosner, L. Zhang, R.A. Holt, C.J. Sansonetti, and J.D. Gillaspay: Phys. Rev. Lett. **71**, 2188 (1993)
12. T.P. Dinneen, N. Berrah-Mansour, H.G. Berry, L. Young, and R.C. Pardo: Phys. Rev. Lett. **66**, 2859 (1991)
13. E.G. Myers, D.J.H. Howie, J.K. Thompson, and J.D. Silver: Phys. Rev. Lett. **76**, 4899 (1996)
14. J.K. Thompson, D.J.H. Howie, and E.G. Myers: Phys. Rev. A**57**, 180 (1998)
15. E.G. Myers, H.S. Margolis, J.K. Thompson, M.A. Farmer, J.D. Silver, and M.R. Tarbutt: Phys. Rev. Lett. **82**, 4200 (1999)
16. E.G. Myers, P. Kuske, H.J. Andr , I.A. Armour, N.A. Jelley, H.A. Klein, J.D. Silver, and E. Traebert: Phys. Rev. Lett.**47**, 87 (1981); E.G. Myers: Nucl. Instrum. Methods Phys. Res., Sect. B **9**, 662 (1985)
17. D.J.H. Howie, J.D. Silver, and E.G. Myers: J. Phys. B**29**, 927 (1996)
18. K.W. Kukla, A.E. Livingston, J. Suleiman, H.G. Berry, R.W. Dunford, D.S. Gemmell, E.P. Kanter, S. Cheng, and L.J. Curtis: Phys. Rev. A**51**, 1905 (1995)
19. B.B. Birkett, J.-P. Briand, P. Charles, D.D. Dietrich, K. Finlayson, P. Indelicato, D. Liesen, R. Marrus, and A. Simionovici: Phys. Rev. A **47**, R2454 (1993)
20. P. Indelicato, B.B. Birkett, J.-P. Briand, P. Charles, D.D. Dietrich, R. Marrus, and A. Simionovici: Phys. Rev. Lett. **68**, 1307 (1992)

21. E.G. Myers and M.R. Tarbutt: Phys. Rev. A **61**, 10501(R) (1999)
22. A.G. Maki, C.C. Chou, K.M. Evenson, L.R. Zink, and J.T. Shy: J. Mol. Spec. **167**, 211 (1994)
23. L.C Bradley, K.L. Soohoo, and C. Freed: IEEE J. Quant. Elect., QE-22, 234 (1986)
24. W.R. Johnson, D.R. Plante and J. Sapirstein: Adv. At. Mol. Opt. Phys. **35**, 255 (1995)
25. J.F. Ziegler: *Stopping Cross-Sections For Energetic Ions In All Elements*, Pergamon Press, New York (1980)
26. H.A. Klein, F. Moscatelli, E.G. Myers, E.H. Pinnington, J.D. Silver, and E. Traebert: J. Phys. B. **18**, 1483 (1985)
27. D.R. Plante, W.R. Johnson, and J. Sapirstein: Phys. Rev. A **49**, 3519 (1994)
28. M.H. Chen, K.T. Cheng, and W.R. Johnson: Phys. Rev. A **47**, 3692 (1993)
29. G.W.F. Drake: Can. J. Phys. **66**, 586 (1988)
30. S.A. Lewis, F.M.J. Pichanick, and V.W. Hughes: Phys. Rev. A **2**, 86 (1970)
31. W. Frieze, E.A. Hinds, V.W. Hughes, and F.M.J. Pichanick: Phys. Rev. A **24**, 279 (1981)
32. G.W.F. Drake: private communication 1999
33. D.J.H. Howie, W.A. Hallett, E.G. Myers, D.D. Dietrich, and J.D. Silver: Phys. Rev. A **49**, 4390 (1994)
34. W. Curdt, E. Landi, K. Wilhelm, and U. Feldman: Phys. Rev. A **62**, 22502 (2000)
35. R. DeSerio, H.G. Berry, R.L. Brooks, J. Hardis, A.E. Livingston, and S.J. Hinterlong: Phys. Rev. A **24**, 1872 (1981)
36. D.J.H. Howie, J.D. Silver, and E.G. Myers: Phys. Rev. A **52**, 1761 (1995)
37. J.P. Buchet, M.C. Buchet-Poulizac, A. Denis, J. Desesquelles, M. Druetta, J.P. Grandin, and X. Husson: Phys. Rev. A **23**, 3354 (1981)
38. S. Martin, A. Denis, M.C. Buchet-Poulizac, J.P. Buchet, and J. Desesquelles: Phys. Rev. A **42**, 6570 (1990)